A high-intensity, pulsed supersonic carbon source with $C(^3P_j)$ kinetic energies of 0.08–0.7 eV for crossed beam experiments

R. I. Kaiser and A. G. Suits
Department of Chemistry, University of California and Chemical Sciences Division, Lawrence Berkeley National Laboratory, Berkeley, California 94720

(Received 24 July 1995; accepted for publication 19 September 1995)

An enhanced supersonic carbon source produces carbon atoms in their $C(^3P_j)$ electronic ground states via laser ablation of graphite at 266 nm. The 30 Hz (40±2) mJ output of a Nd-YAG laser is focused onto a rotating graphite rod with a 1000 mm focal length UV-grade fused silica plano-convex lens to a spot of (0.5±0.05) mm diameter. Ablated carbon atoms are subsequently seeded into helium or neon carrier gas yielding intensities up to 10^{13} C atoms cm^{-3} in the interaction region of a universal crossed beam apparatus. The greatly enhanced number density and duty cycle shift the limit of feasible crossed beam experiments down to rate constants as low as 10^{-11}–10^{-12} $cm^3\ s^{-1}$. Carbon beam velocities between 3300 and 1100 m s^{-1}, with speed ratios ranging from 2.8 to 7.2, are continuously tunable on-line and *in situ* without changing carrier gases by varying the time delay between the laser pulse, the pulsed valve, and a chopper wheel located 40 mm after the laser ablation. Neither electronically excited carbon atoms nor ions could be detected within the error limits of a quadrupole-mass spectrometric detector. Carbon clusters are restricted to ~10% C_2 and C_3 in helium, minimized by multiphoton dissociation, and eliminating the postablation nozzle region. © *1995 American Institute of Physics.*

I. INTRODUCTION

Chemical reactions of ground state atomic carbon $C(^3P_j)$ play a major role in combustion processes,[1–3] hydrocarbon syntheses,[1–3] and interstellar chemistry.[4–8] However, predominantly energy-dependent reaction cross sections, product distributions, and branching ratios are extracted from bulk experiments in flow cells and static gas cells.[9,10] This approach cannot eliminate three-body collisions and biases a detailed picture of each reaction by stabilization of vibrationally and/or electronically excited reaction complexes or unstable intermediates. On the other hand, seeding of $C(^3P_j)$ in carrier gases generates an intense supersonic carbon beam. Performing a crossed beam experiment with the second reactant in combination with time- and angular-resolved product detection via a quadrupole mass spectrometer elucidates detailed information on elementary steps in chemical reactions.[11,12]

Owing to the $C(^3P_j)$ enthalpy of formation of 716.49 kJ mol^{-1} (Ref. 13) and its reactivity, a beam of supersonic carbon atoms is troublesome to produce. Two approaches are possible: *external* coupling of a large amount of energy into the $C(^3P_j)$ precursor or synthesizing energetic precursors with masked carbon atoms (*internal* or *chemical* energy).

Molecules storing a huge amount of energy in their enthalpy of formation, e.g., 5-tetrazoyldiazonium chloride (1) or tetracyclo[3.2.0.$0^{2,7}$.$0^{4,6}$]-heptane-3-ylidene-tosylhydrazone lithium salt (2) widely served as carbon sources.[2,14,15] Heating of (1) and (2) releases nitrogen, hydrogen chloride, and atomic carbon (1) or carbon and benzene (2), respectively. Actually, precursor (1) is extremely unstable: preparation is limited to 0.76 mmol and even etheric solutions are explosive at 200 K standing for less than 1 h.[14,15] Precursor (2) undermines the purpose of molecular beam studies: carbon atoms react with benzene yielding a messy supersonic beam.

Wolf,[16] Wolfgang,[17] and Stöcklin[18] initiate ^{11}C and ^{14}C recoils by nuclear reactions, e.g., implanting protons or neutrons into gaseous nitrogen, i.e., $^{14}N\ (n,p)\ ^{14}C$, and $^{14}N\ (p,\alpha)\ ^{11}C$. But as a consequence of multiple elastic/inelastic energy transfers in binary encounters of keV recoil carbons with target molecules,[19] only a broad energy distribution with $\Delta v/v \geqslant 0.2$ (v = root mean square velocity, Δv = intensity at half-maximum of velocity distribution) is achieved. In addition, the number density of recoil carbon atoms is restricted to 10^7–10^8 cm^{-3} in the source region, up to six orders of magnitude too low for feasible crossed beam applications.

Alternatively, irradiation of pyrolytic graphite at 1800–2500 K with keV noble-gas ions (radiation enhanced sublimation) generates predominantly atomic carbon when bombarded with 5 keV Ar^+ ions, with the formation of only minor amounts of C_2 (C_1/C_2=25–40 at 2100 K).[20–24] However, adaptation to molecular beams reveals the shortcomings of this method: typically, sputter yields of <5 carbon atoms per Ar^+ ion are achieved. Assuming a maximum Ar^+ values of 3×10^{15} $cm^{-2}\ s^{-1}$ of commercially available ion guns impinging to an area of ~10 mm^2 and experimentally determined peak velocities of 10^3–10^4 m s^{-1}, an upper number density of 10^{11} C cm^{-3} in the source region is provided before supersonic expansion takes place, thus, it is too low to be applied in crossed beam experiments.

Another approach consists of placing an arc between two graphite electrodes, vaporizing graphite at 2500–3500 K.[25] The vapor is either seeded in a carrier gas or reacts directly with the surrounding target molecules. In spite of the number densities up to 10^{18} C atoms cm^{-3}, the production of larger carbon clusters up to C_5 as well as irreproducible electrode-

 0034-6748/95/66(12)/5405/7/$6.00

surface conditions yield unstable sublimation rates and complicate this procedure.

Photolysis of carbon suboxide, C_3O_2, releases carbon atoms in their first excited ^1D ($\lambda<172$ nm) or ground ^3P ($\lambda<207$ nm) state.[26–33] The carbon suboxide precursor, however, polymerizes even at 77 K, decomposes randomly during sublimation purification,[34] and yields electronically excited C_2O in the supersonic beam, interfering with reactions of carbon atoms. Attempts have been worked out to overcome C_2O ($^3\Sigma^-$, $^1\Delta$) by two-photon dissociation, but low absorption cross sections limit the desired success.

Similarly, radio frequency and microwave discharges of He/CH_4 flow systems produce carbon atoms as well as ions.[3] Unavoidable CH and CH_2-radical by-products complicate possible applications in crossed beam techniques. Last, neutralization of accelerated carbon ions to 2–5000 eV by charge exchange on tungsten wires or graphite yields carbon atoms. Space charge effects, however, limit the number density in the regime of "chemical energies" ($E<10$ eV) to 10^{14} C atoms cm^{-3} in the source region.[1,2]

Among the great variety of approaches, laser ablation of graphite is a promising candidate to yield a high intensity, stable and reproducible supersonic carbon source to be employed in crossed beam experiments. In 1985, Costes *et al.*[35,36] developed a pulsed supersonic carbon beam source based on Smalley and co-worker's laser-vaporization supersonic nozzle source.[37] Carbon atoms were generated by laser ablation of graphite at 248 nm (KrF excimer) or 266 nm (fourth harmonic of a Nd-YAG). A Gentry–Giese pulsed valve operating at 10 Hz entrains laser-ablated carbon atoms in the helium carrier gas to gain supersonic carbon-atom velocities of 2140 m s^{-1} with $\Delta v/v=0.1$–0.2. Minimization of $C_2(^1\Sigma_g^+)$ and C_3 ($^1\Sigma_g^+$) was achieved by reducing the downstream channel length to 2 mm and, consequently, the downstream dwell time of ablated species to <2 μs. Reisler *et al.*'s design[38,39] matches Costes' carbon source, but yields velocities between 1270 and 1790 m s^{-1} with $\Delta v/v\approx0.2$ and 70 000 m s^{-1} ($\Delta v/v=1$; free ablation).

Both designs, however, drive the pulsed valve and laser with only 10 Hz; if shot-to-shot background subtraction is desired, the repetition rate of the Nd:YAG laser drops to 5 Hz. Additionally, number densities are limited to $<10^{12}$ C atoms cm^{-3} in the interaction region. Both limitations constrain crossed beam reactions to rate constants of $k>10^{-10}$ cm^3 s^{-1}, reactions with smaller rate constants are hardly accessible with common setups. Further, current designs cannot tune the velocity of the supersonic-carbon beam continuously: this deficit, however, limits the versatility and resolution to determine energy-dependent cross sections and threshold energies for endothermic reactions. The carbon pulse duration is very long and no time zero for time-of-flight or laser-induced fluorescence data recording is provided. Finally, quantitative distributions of carbon clusters have not been elucidated.

Therefore, the new generation of supersonic carbon sources to be constructed has to fulfill the following requirements: (a) number densities of $>10^{12}$ C atoms cm^{-3} in the interaction region; (b) minimization of carbon clusters; (c) quantitative determination of the ratio of carbon clusters to atomic carbon; (d) exclusion of carbon ions; (e) tunable, reproducible, and long-term stability of the supersonic carbon beam; (f) increasing the duty cycle; and (g) very short beam pulse to provide precise time origin. Finally, the lifetime of $C(^1D_j)$ and $C(^1S_j)$, i.e., 53 ms and 2 s, respectively, versus typical flight times of carbon atoms from the laser-ablation zone to the interaction region in the μs regime enforces the elimination of electronically excited carbon atoms(h).

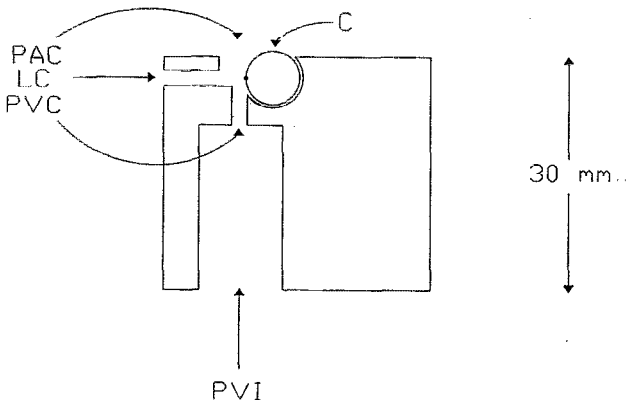

FIG. 1. Schematic top view of the aluminum block of the carbon source: C: carbon rod; PVI: pulsed valve insert; LC: laser beam channel: PVC: pulsed valve extension channel; PAC: postablation extension channel. ● indicates the ablation region.

The article is laid out as follows: Sections II A–II C describe the experimental setup, i.e., the design of the carbon source and incorporation into the vacuum system, the carbon beam generation, and data acquisition. The results focus on velocities and speed ratios of the supersonic carbon beam, beam composition, and number densities in the interaction region (Secs. III A–III C). Finally, the discussion in Sec. IV centers on specified demands (a)–(h).

II. EXPERIMENTAL SETUP

A. Design of the carbon source

The center of the carbon source is made of a (30 mm×40 mm×15 mm) aluminum block, Fig. 1, attached to a stainless steel frame with (50 mm×50 mm×300 mm) dimensions. Carbon rods, of SPK purity grade with <2 ppm ash content, are supplied by Bay Carbon Inc., MI, and were turned down to 1.06 cm o.d. limited by the thermal expansion induced by the laser irradiation. The carbon rod is located 0.1 mm inside the extension channel of a Proch–Trickl pulsed valve with a 0.75-mm-i.d. nozzle.[40] The pulsed valve extension channel, of 1 mm i.d., extends 8 mm from the valve to the laser ablation region and intersects the 2-mm-diam laser hole channel at 90°. The encountered carbon rod is interfaced to an Oriel dc motor, type 18078, and is kept in a helical motion during the laser irradiation. This design guarantees bidirectional repeatability motion with high vertical and horizontal precision over a 45 mm travel length. Wobbling effects of the carbon rod are eliminated completely. A contact plate coupling the carbon rod to the motor tip triggers polarity switch of the motor via a bistable relay (Philips ECG RLY7742, 12 V dc, 15 A) after hitting a microswitch. Optionally, the polarity switch can be induced by

an external timer circuit. This integrated feedback system maintains a constant speed in either direction, which is necessary for shot-to-shot reproducibility for laser ablation of graphite. The postablation extension channel was limited to 1 mm length and opened to 6 mm i.d.; longer channels, reduced diameters, and conelike extensions were found to clog after 1–2 operation hours even at low laser powers of 5 mJ per pulse. The modular design of the carbon source, i.e., the aluminum block, the stainless steel frame, and the pulsed-valve holder, allows interfacing this construction to an x-translation stage: a vacuum feedthrough manipulates the nozzle–skimmer distance and optimizes the carbon concentration at a given laser power. Additionally, moving the stainless steel frame 60 mm away from the skimmer permits changing of the carbon rod without interfering with the alignment of the source.

B. Incorporation of the carbon source in the vacuum system

The optimization of the carbon source is performed in a modified universal crossed molecular beam apparatus described in detail in Ref. 41. Briefly, the 30 Hz (40±2) mJ per pulse, 266 nm output of a Spectra Physics GCR-270-30 Nd:YAG laser is focused on the carbon rod with a 1000 mm focal length UV-grade fused silica plano-convex lens to a spot of (0.5±0.05 mm o.d. after passing through a UV-grade fused silica window. This arrangement restricts the beam absorption to (4.0%±0.5%). The laser beam entrance channel is completely isolated from the second source region to avoid reaction of carbon atoms in the first source with background reactant molecules. The pulsed supersonic beam of carbon atoms (source I) and the second reactant, i.e., a continuous supersonic acetylene beam in our test experiments, (source II) pass through skimmers with apertures of 1.0 and 0.58 mm, attached to a differential wall to reduce the background in the reaction chamber, which is typically held at 1×10^{-7} Torr (Fig. 2) and cross at 90° with divergences of 3.0° and 4.3°, respectively. The Proch–Trickl pulsed valve operates at 60 Hz, 80 μs pulses, and 4 atm backing pressure of helium and is driven by −500 V pulses. The continuous source in region II features a 0.1 mm nozzle diameter, and a backing pressure of (563±6) Torr acetylene (Matheson, 99.5%) purified by an acetone absorber and an acetone–dry ice cold trap. Likewise, the nozzle-interaction region distance was optimized to (61.2±0.1) mm and (27.0±0.1) mm (the first source and second source, respectively).

The supersonic carbon beam or reactively scattered species was monitored using a triply differentially pumped ultrahigh vacuum (UHV) chamber, rotatable in the plane of the beams with respect to the interaction region with dimensions of (3.2 mm×3.2 mm×3.2 mm). Each region is evacuated by an ion pump and a magnetic suspended turbomolecular pump, yielding $\sim4\times10^{-11}$ Torr in the third region. All turbomolecular pumps are backed by an oil-free Drytel pump. A slide valve with a 4-mm-i.d. O-ring is used to separate the reaction chamber from the first differentially pumped detector region: During on-axis operation a small detector aperture of 0.23 mm i.d. is used, whereas off-beam-axis reactive scattering experiments require a larger, 3.8 mm×3.8 mm

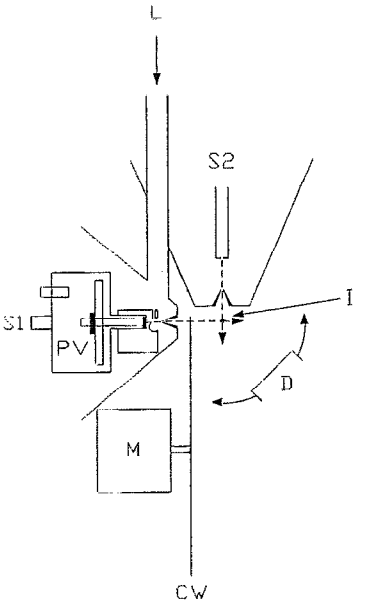

FIG. 2. Schematic top view of the crossed molecular beam setup: D: detector; I: interaction region; S1: source 1; S2: source 2; PV: pulsed valve; L: laser; M: motor; CW: chopper wheel. The reactant beams (dashed lines) intersect in the interaction region at 90°.

rectangular aperture. Differentially pumped chamber I serves to reduce the gas load from the main chamber, whereas chamber II evacuates the quadrupole mass filter, and the Daly-type scintillation particle detector.[42] Chamber III contains the Brink-type ionizer (ionization efficiency of $\sim10^{-4}$ at 10 mA emission current),[43] surrounded by a liquid nitrogen cold shield. Two (5.8 mm×5.8 mm) rectangles constrain the viewing angle of the ionizer nested 34.5 cm from the interaction region to 1.7° in each direction. The ionizer consists of a carbon-coated thoriated tungsten filament spot welded to a gold-plated stainless steel cylindrical can, a meshed wire grid, and an extractor lens held at −800 V. The electron energy, i.e., the potential difference between the can and the grid, was optimized to 200 eV, whereas the ion energy was held at +80 eV (the potential difference between the grid potential and grounded quadrupole rod system). Extracted ions are focused by an electric lens located after the extractor plate, past the quadrupole mass filter, and are accelerated toward a stainless steel target maintained at −25 kV. The ion hits the surface and initiates an electron cascade; the electrons are accelerated by the same potential until they reach an organic scintillator whose photon cascade is detected by a photomultiplier (PMT) mounted outside the UHV detector and held between 1200 and 1700 V. The count rate is limited to 1 MHz to avoid saturation, i.e., overlapping recharge intervals of capacitors in the dynode chain. Each PMT pulse is amplified in a dual linear amplifier (LRS, model 133B) and passes a discriminator (LRS, model 621 BL) to suppress low-level noise. After converting from a NIM to a transistor–transistor logic (TTL) standard by a level adapter (LeCroy, model 688AL), the signal is fed into two home-built multichannel scalers—MCS I and II (the dwell time of the channel between 1 and 7.5 μs). This setup enables us to record either a standard mass spectrum, i.e., scanning a predefined range of mass-to-charge ratios of

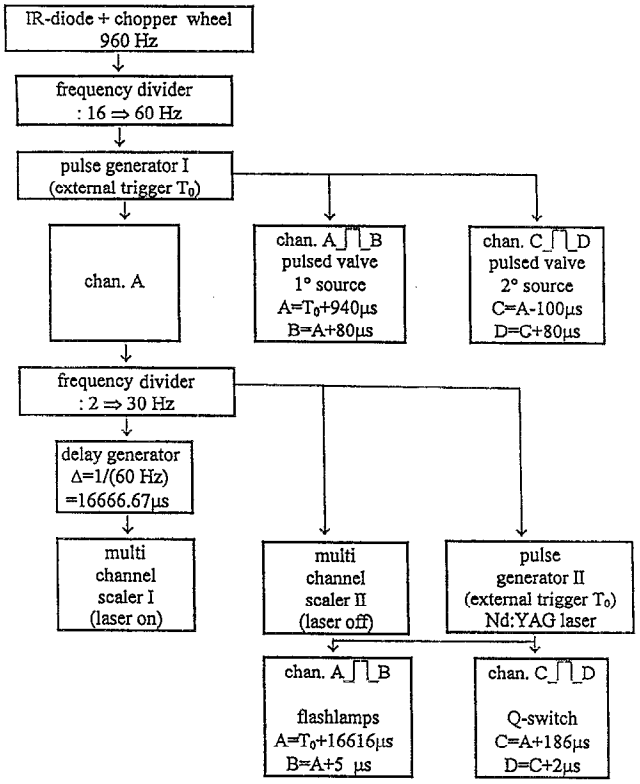

FIG. 3. Pulse sequence in the crossed beam experiments. Optionally, the pulsed valve II can be replaced by a continuous source.

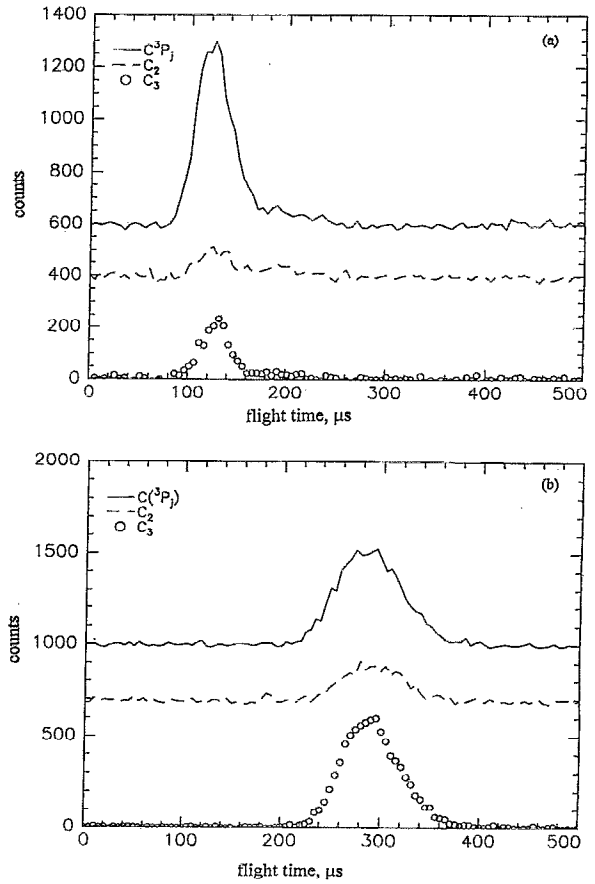

FIG. 4. Time-of-flight-spectra of $m/z=12$ (C^+), 24 (C_2^+), and 36 (C_3^+), recorded with 80 eV electron energy: (a) parameter set 3, Table I; (b) parameter set 4, Table II.

transmitted ions versus their intensity by increasing the dc voltage applied to the quadrupole rods, or a TOF spectrum, i.e., the time-dependent intensity of ions with *one m/e* ratio.

C. Carbon-beam generation and data acquisition

TOF spectra of the supersonic carbon beam were recorded on-axis choosing the small detector aperture, cf. Sec. II B. A chopper wheel of 17.8 mm diam with four 8-mm-long and 1-mm-wide slots located 90° apart is attached to a synchronous three-phase motor (model 75A1004-2, Globe Motors) and spins at 240 Hz. The 960 Hz TTL output of an IR diode (Newark Electronics, type OPB960, configuration T) mounted at the top of the motor-supporting frame is coupled into a frequency divider (division by 16), yielding a 60 Hz external TTL trigger pulse for pulse generator I (SRS, model 535), cf. Fig. 3. The 940 μs delayed TTL output of channel AB (pulse width=80 μs) triggers the pulsed valve I in the primary source. In the case of reactive scattering experiments and a pulsed source II, pulsed valve II is triggered at 100 and 102 μs—C_2H_2-reactant molecules—prior to the triggering of pulsed valve I. This timing sequence limits the depletion of the carbon beam to (17.5%±0.5%) and, thus, limits three-body collisions in the interaction region to <3%. A second frequency divider reduces the output of channel A to 30 Hz, triggering (a) a MCS I of 16 666.67 μs after the initial pulse, (b) MCS II, and (c) pulse generator II (SRS, model 535). The TTL output of channel AB ignites flash lamps of the Nd:YAG laser 16 616 μs after the helium or—alternatively—16 618 μs after a neon pulse (4 atm neon backing pressure), whereas the CD–TTL output opens the Q-switch 186 μs time delayed. Raw data are accessed via a 6001 crate controller (DSPT), interfaced to a 486DX-PC. The present trigger sequence records TOF spectra with "laser on" (MCS I) and "laser off" to enable pulsed valve modulated background subtraction for alternate triggers (MCS II).

III. RESULTS

A. Velocity and speed ratio of the carbon beam

Figure 4 displays typical TOF spectra of $m/z=12$ (C^+), 24 (C_2^+), and 36 (C_3^+), recorded with 80 eV electron energy, after optimization of the experimental parameters, i.e., pulse and delay sequences, helium backing pressure, pulsed valve pulse width, dimensions of the carbon source, the laser power, and the distance the nozzle–interaction region contributes to points (a)–(g), cf. Sec. I. The velocity of C_1, C_2, and C_3 were determined by fitting the TOFs after offset correction, i.e., electronic offset (the difference between the MCS trigger pulse and IR-diode pulse, the response time of MCS I and the IR diode, the MCS I offset of channel AB with respect to $t=1/60$ s), physical offset (misalignment of the chopper wheel and IR diode), and ion-flight time[44,45] to

TABLE I. Typical characteristics of the carbon beam in crossed beam experiments.

Set	Seeding gas	Velocity ($m\ s^{-1}$)	Speed ratio	$C_1:C_2:C_3$
1	He	3272±55	2.81±0.1	1:(0.04±0.02):(0.2±0.1)
2	He	2518±10	4.65±0.1	1:(0.1±0.05):(0.25±0.05)
3	He	2340±58	7.3±0.4	1:(0.06±0.04):(0.07±0.04)
4	Ne	1177±3	6.4±0.05	1:(0.7±0.1):(2.5±0.3)

$$N(v)=v^2\exp\left[-\left(\frac{v}{\alpha}-S\right)^2\right] \tag{1}$$

after convolution over the ionizer length and the shutter function of the chopper wheel. The number density of molecules with velocity v, $N(v)$, is given as a function of two additional parameters, the speed ratio S and $\alpha=m/2RT$, where m is the mass of the molecule (atom), T the temperature of the beam, and R the ideal gas constant. This fitting routine yields supersonic velocities of the seeded carbon atoms to, e.g., $v_{(C/He)}=(2340\pm58)$ m s^{-1} and a speed ratio of $S=(7.3\pm0.2)$, averaged over one month experimental time. Varying the delay times of pulsed valve I allows a continuously tunable helium seeded carbon-beam velocity from 2100 to 3300 m s^{-1} with velocity fluctuations less than 4%, cf. Table I. Speed ratios increase with reduced carbon-beam velocity from 2.81±0.1 (3272±55 ms^{-1}) to 7.3±0.4 (2340±58 m s^{-1}). Higher velocities up to 3800 m s^{-1} are available, but He–Rydberg atoms formed in the ablation interfere with measurements. The low-velocity cutoff of ~2100 m s^{-1} is governed by decreasing carbon beam intensity down to ~10% of the peak intensity. Lower velocities between 1800 and 1100 m s^{-1}, however, are archived by varying the seeding gas to neon (99.995%, Matheson gas). The excluded velocity regime of 2100–1800 m s^{-1} is accessible via seeding carbon atoms in He/Ne mixtures.

B. Composition of the carbon beam

The carbon beam is characterized by performing on-axis TOF measurements between $m/z=12$ (C^+), and 120 (C_{10}^+) in $m/z=12$ increments at an emission current of 4 mA and an electron kinetic energy of 80 eV. Results show cluster production restricted to C_2 and C_3, if a laser power of >10 mJ per pulse at 266 nm, i.e., $>10^{13}$ W m^{-2}, is applied. Predominantly, multiphoton dissociation destroys larger carbon clusters. The ratio of $C_1:C_2:C_3$ was determined by (a) integrating TOF of $m/z=12$ (C^+), 24 (C_2^+), and 36 (C_3^+), (b) correcting for the relative ionization cross section, and (c) accounting for fragmentation pattern of cations formed in the ionizer region. In the case of closed shell species without structural isomers, the ionization cross sections σ_{ion} scales with the square root of the molecular polarizability α[46] within ±20%:

$$\sigma_{ion}=36\sqrt{\alpha}-18, \tag{2}$$

whereas the molecular polarizability is calculated as the sum of atomic polarizabilities, i.e., yielding $\sigma_{(C_1)}:\sigma_{(C_2)}:\sigma_{(C_3)}$ = 1: (1.5±0.2):(1.8±0.3). Krajnovich determined cracking patterns of the carbon clusters at 80 eV electron energy and yielded ~33% fragmentation of C_3^+ to C^+ and C_2, as well as ~30% fragmentation of C_2^+ to C^+ and C.[47] Correcting for this, we find relative number densities $C_1:C_2:C_3=1$: (0.06 ±0.04):(0.07±0.04) at a velocity of (2340±58) ms^{-1}. Changing from helium to neon seeding gas increases cluster production from ~20% to 70%, cf. Table I.

In addition, carbon and cluster ions were probed by (a) turning the emission current of the ionizer-filament off and grounding the grid, and (b) performing reactive scattering with C_2H_2 with and without an external electric field of $E=300$ V cm^{-1}, however, no C_n^+ ions could be detected. Moreover, electronically excited carbon atoms were probed in a reactive scattering experiment of helium seeded carbon atoms with molecular hydrogen: the reaction of $C(^3P_j)$ with H_2 is endothermic by 92.4 kJ mol^{-1} and does not produce CH radicals sampled as CH^+ at $m/z=13$:

$$H_2(^1\Sigma_g^+)+C(^3P_j)\rightarrow CH(^2\Pi_j)+H(^2S_{1/2});\quad \Delta_R G^0=+92.4\ \text{kJ mol}^{-1}, \tag{3}$$

$$H_2(^1\Sigma_g^+)+C(^1D_j)\rightarrow CH(^2\Pi_j)+H(^2S_{1/2});\quad \Delta_R G^0=-33.3\ \text{kJ mol}^{-1}, \tag{4}$$

$$H_2(^1\Sigma_g^+)+C(^1S_j)\rightarrow CH(^2\Pi_j)+H(^2S_{1/2});\quad \Delta_R G^0=-167.4\ \text{kJ mol}^{-1}. \tag{5}$$

On the other hand, $C(^1D_j)$ and $C(^1S_j)$ yield $CH(^2\Pi_j)$. Nevertheless, not even traces of electronically excited carbon atoms could be detected. Further checks were performed by inelastic scattering of $C(^1D_j)$ with xenon atoms with a quenching rate at 293 K, $k=(1.1\pm0.3)\times10^{-10}$ $cm^3\ s^{-1}$. Likewise, no inelastic energy processes were observed and eliminate carbon in its $C(^1D_j)$ and $C(^1S_j)$ state.

C. Number density of carbon atoms in the interaction region

After a few nozzle diameters, the supersonic flow expands radially from the nozzle treated as a virtual point source.[48] In the absence of an interaction between the Mach disk and the supersonic expansion, the on-axis ($\Theta=0$) number density $n(R,\ \Theta=0)$ at a distance R, with the nozzle diameter D and the postnozzle distance R hold the relation

$$n(R,\ \Theta=0)=fn_0(R/D)^{-2}, \tag{5}$$

with a scaling parameter f ($f=0.15$ for monoatomic gases) and the number density in the source region n_0. The radial dependence at constant R is given by

$$n(R,\Theta)=n(R,0)\cos^2(s\Theta) \tag{6}$$

with an angular scaling parameter s ($s=1.15$ for monoatomic gases). Using a known number density of helium atoms as a calibrant at 4 atm backing pressure at 293 K, the number density of carbon atoms in the interaction region can be calculated. Including the different ionization cross sections of helium and carbon of $\sigma_{(He,\ 200\ eV)}:\sigma_{(C,\ 200\ eV)}=3.7\times10^{-17}$ cm^{-2}:1.7×10^{-16} cm^{-2},[49] a number density of $(0.7\pm0.3)\times10^{13}$ cm^{-3}, i.e., (0.3%±0.1%) carbon atoms seeded in helium, in the interaction region, is derived.

TABLE II. Characteristics of currently operating carbon sources in crossed beam experiments.

Wavelength, (nm)	Length and diameter upstream channel (mm)	Length and diameter downstream channel (mm)	Pulse energy (mJ)	Downstream dwell time (μs)[c]	Gas volume per pulse (mm^3)	(%C)	FWHM, gas pulse (μs)	Repetition rate pulsed valve, and laser (Hz)	C_1:C_2:C_3	Helium backing pressure (atm)	Velocity (ms^{-1})	$\Delta v/v$	Reference
248	8,[a] 1	8,[a] 1	10	2	8	<0.9[b]	10	10, 10	Not determined	10	2140	0.1–0.2	35, 36
266	8, 1	8,[a] 1	25	2	8	<2.3[b]	10	10, 10	Not determined	10	2140	0.1–0.2	35, 36
266	?	?	3.5	?	40	<1.1[b]	50	10, 10	Not determined	7.5	1270–1790	0.2[d]	33, 34
							...	–, 10		...	70 000	1[e]	
266	8, 1	...	38±2	...	36	0.7±0.3	80	60, 30	1: (0.06±0.04): (0.07±0.04)	4	3300–1100	<0.15	Present work

[a]Last 6 mm: 90° cone.
[b]Estimated.
[c]The pumping speed S through nozzle with nozzle diameter d is given by $S=\pi(d/2)^2 v$ with the velocity of a gas with molecular mass m at temperature T in the pulsed valve extension channel $v=\sqrt{\gamma RT/m}$, whereas γ is defined as the ratio of specific heats at constant pressure and volume, respectively, i.e., $\gamma=c_{mp}/c_{mV}$. The residence time t of ablated carbon atoms in downstream extension nozzle with volume V is calculated by $t=V/S$.
[d]Seeded ablation.
[e]Free ablation.

IV. DISCUSSION

A comparison of our operation conditions and specifications with Table II, compiling characteristics of currently operating carbon sources in crossed beam experiments, underlines the novel features of the newly designed carbon source combined with a quadrupole mass spectrometer and a chopper wheel. The continuously tunable velocity regime extends from 3300 to 1100 m s^{-1} with standard deviations of less than 5% and, therefore, enlarges the experimentally accessible range by 1200 m s^{-1} (high velocity limit) and 200 ms^{-1} (low velocity limit), i.e., yielding collision energies in reactive scattering experiments with, e.g., acetylene (v=866 ms^{-1}), between 8 and 48 kJ mol^{-1}. Additionally, the increased repetition rates of the laser from 10 to 30 Hz improve the duty cycle by a factor of 3. Taking into consideration the higher number density of carbon atoms in the interaction region of $(0.7\pm0.3)\times10^{13}$ cm^{-3} vs $<10^{12}$ cm^{-3} in Refs. 35, 36, 38, and 39, reactive scattering signals increase at least by 30-fold. Therefore, the lower limit of feasible crossed beam experiments decreases to rate constants in the 10^{-11}–10^{-12} cm^3 s^{-1} domain. Seeding gases, however, should be restricted to helium and neon to avoid cluster growth at the expense of atomic carbon: helium limits cluster contribution to 10%–25% of C_n species, whereas the clustering in neon expands up to 75%.

Moreover, the new carbon source determines the composition of the carbon-beam on line and *in situ*: operation parameters were optimized by minimizing carbon clusters detectable via LIF, whereas the present setup allows beam monitoring, i.e., composition and velocity, to endure a long-term stable supersonic carbon beam. Currently, reproducible beam characteristics are accomplished ablating single carbon rods up to 340 h. Minor drifts during the experiments and intensity fluctuations are compensated by varying the delay time of the pulsed valve and the laser, i.e., picking a different part of the gas pulse, and adjusting the focus of the 1000 mm lens onto the rotating carbon rod. Further, characterization of the carbon beam depicts a complete absence of electronically excited carbon atoms and ions.

In summary, the present, modular design of the carbon source will gain an enormous boost in the reaction dynamics of carbon atoms as well as other refractory elements via crossed beam experiments. Threshold energies for endothermic reactions, for example, can be simply elucidated by tuning the carbon-beam velocity. Future projects are aimed at extending the energy regime by increasing the wheel frequency to 400 Hz, reducing the slot width from 1 to 0.1 mm and performing a free ablation: only a 0.4 μs window of a free-ablation carbon pulse is transmitted. Preliminary experiments limit the velocity regime to ≈8.5 eV.

ACKNOWLEDGMENTS

One of us (R.I.K.) is indebted to the Deutsche Forschungsgemeinschaft for a postdoctoral fellowship. Both of us would like to thank Professor H. Reisler, USC, for valuable discussions regarding the carbon source. This work was supported by the Director, Office of Energy Research,

Office of Basic Energy Sciences, Chemical Sciences Division of the U.S. Department of Energy under Contract No. DE-AC03-76SF00098.

[1] *Reactive Intermediates in the Gas Phase,* edited by D. W. Setser (Academic, New York, 1979).
[2] *Reactive Intermediates*, edited by R. A. Abramovich (Plenum, New York, 1980).
[3] *Short-Lived Molecules*, edited by M. J. Almond (Harwood, New York, 1990).
[4] K. Roessler, H. J. Jung, and B. Nebeling, Adv. Space Res. **4**, 83 (1984).
[5] K. Roessler, Radiat. Eff. **99**, 21 (1986).
[6] R. I. Kaiser, R. M. Mahfouz, and K. Roessler, Nucl. Instrum. Methods B **65**, 447 (1992).
[7] E. Herbst, H. H. Lee, D. A. Howe, and T. J. Millar, Mon. Not. R. Astron. Soc. **268**, 335 (1994).
[8] T. J. Millar and E. Herbst, Astron. Astrophys. **288**, 561 (1994).
[9] A. J. Dean, D. F. Davison, and R. K. Hanson, J. Phys. Chem. **95**, 183 (1991).
[10] W. Braun, A. M. Bass, D. D. Davis, and J. D. Simmons, Proc. R. Soc. London Ser. A **312**, 417 (1969).
[11] G. Scoles, *Atomic and Molecular Beam Methods* (Oxford University Press, New York, 1988), Vol. 1.
[12] Y. T. Lee, in Ref. 11, p. 553.
[13] *Handbook of Chemistry and Physics*, edited by D. R. Lide (Chemical Rubber, Boca Raton, FL, 1993).
[14] P. B. Shevlin, J. Am. Chem. Soc. **94**, 1379 (1972).
[15] M. L. McKee, G. C. Paul, and P. B. Shevlin, J. Am. Chem. Soc. **112**, 3374 (1990).
[16] A. P. Wolf, Adv. Phys. Org. Chem. **2**, 201 (1964).
[17] R. Wolfgang, Prog. React. Kinet. **3**, 97 (1965).
[18] G. Stöcklin, *Chemie heisser Atome* (VCH, Weinheim, 1969).
[19] W. Eckstein, *Computer Simulation of Ion–Solid Interaction* (Springer, Berlin, 1991).
[20] V. Philipps, K. Flaskamp, and E. Vietzke, J. Nucl. Mater. **111/112**, 781 (1982).
[21] E. Vietzke, V. Philipps, K. Flaskamp, J. Winter, and S. Veprek, J. Nucl. Mater. **176/177**, 481 (1990).
[22] V. Philipps, E. Vietzke, R. P. Schorn, and H. Trinkaus, J. Nucl. Mater. **157**, 319 (1988).
[23] V. Philipps, E. Vietzke, and H. Trinkhaus, J. Nucl. Mater. **179–181**, 25 (1991).
[24] E. Vietzke, K. Flaskamp, M. Hennes, and V. Philipps, Nucl. Instrum. Methods B **2**, 617 (1984).
[25] P. S. Skell, J. S. Havel, and M. J. McGlinchey, Acc. Chem. Res. **6**, 97 (1973).
[26] D. Husain and L. J. Kirsch, Chem. Phys. Lett. **8**, 543 (1971).
[27] D. Husain and L. J. Kirsch, Chem. Phys. Lett. **9**, 412 (1971).
[28] D. Husain and L. J. Kirsch, J. Photochem. **2**, 297 (1973/74).
[29] D. Husain and D. P. Newton, J. Chem. Soc. Faraday Trans. **78**, 51 (1982).
[30] D. Husain and A. N. Young, J. Chem. Soc. Faraday Trans. **71**, 525 (1975).
[31] W. Braun, A. M. Bass, D. D. Davis, and J. D. Simmons, Proc. R. Soc. London Ser. A **312**, 417 (1969).
[32] C. E. M. Strauss, S. H. Kable, G. K. Chawla, P. L. Houston, and I. R. Burak, J. Chem. Phys. **94**, 1837 (1991).
[33] D. C. Scott, J. de Juan, D. Schwartz-Lavi, and H. Reisler, J. Phys. Chem. **96**, 2509 (1992).
[34] H. Reisler (private communication, 1994).
[35] G. Dorthe, M. Costes, C. Naulin, J. Joussot-Dubien, C. Vaucamps, and G. Nouchi, J. Chem. Phys. **83**, 3171 (1985).
[36] M. Costes, C. Naulin, G. Dorthe, G. Daleau, J. Joussot-Dubien, C. Lalaude, M. Vinckert, A. Destor, C. Vaucamps, and G. Nouchi, J. Phys. E **22**, 1017 (1989).
[37] D. E. Powers, S. G. Hansen, M. E. Geusic, A. C. Pulu, J. B. Hopkins, T. G. Dietz, M. A. Duncan, P. R. R. Langridge-Smith, and R. E. Smalley, J. Phys. Chem. **86**, 2556 (1982).
[38] S. A. Reid, F. Winterbottom, D. C. Scott, J. de Huan, and H. Reisler, Chem. Phys. Lett. **198**, 430 (1992).
[39] H. Reisler, in Abstracts of the 17th Combustion Research Contractors Meeting, Wisconsin, 1995 (unpublished).
[40] D. Proch and T. Trickl, Rev. Sci. Instrum. **60**, 713 (1989).
[41] Y. T. Lee, J. D. McDonald, P. R. LeBreton, and D. R. Herschbach, Rev. Sci. Instrum. **40**, 1402 (1969).
[42] N. R. Daly, Rev. Sci. Instrum. **31**, 264 (1960).
[43] G. O. Brink, Rev. Sci. Instrum. **37**, 857 (1966).
[44] M. S. Weis, Ph.D. thesis, University of California, Berkeley, 1986.
[45] M. Vernon, LBL-Report 12422 (1981).
[46] R. E. Center and A. Mandl, J. Chem. Phys. **57**, 4104 (1972).
[47] D. J. Krajnovich (private communication, 1995).
[48] P. C. Engelking, Chem. Rev. **91**, 399 (1991).
[49] K. L. Bell, K. B. Gilbody, and F. J. Smith, J. Phys. Chem. Ref. Data **12**, 891 (1983).